

NANOMETER SCALE COHERENT CURRENT MODULATION VIA A NANOTIP CATHODE ARRAY AND EMITTANCE EXCHANGE *

E. A. Nanni[†], W. S. Graves, MIT, Cambridge, MA, USA
 P. Piot, Northern Illinois University, DeKalb, IL, USA

Abstract

We present particle-in-cell (PIC) simulations of electron bunches with nm scale longitudinal modulation produced using a compact 2-20 MeV LINAC. The modulation is initially imparted in the transverse dimension of the electron bunch with a nano-patterned photo-emitter in an X-band RF gun with 2 MeV exit energy. The electron bunch passes through a 1 m standing wave X-band LINAC which can raise the beam energy up to 20 MeV. The transverse modulation is exchanged into the longitudinal dimension using a double dog-leg emittance exchange setup with a 5 cell RF deflector cavity. The modulation pitch can be tuned by adjusting the spacing of the nano-patterned photo-emitter or magnification of the transverse pitch with electron optics. The electron beam parameters are optimized to produce coherent XFEL radiation upon interacting with a laser undulator.

INTRODUCTION

Inverse Compton scattering (ICS) from a nanostructured electron beam results in the coherent emission of x-rays over a range of wavelengths [1, 2] that are of great interest to the scientific community, as well as a possible seed for a conventional FEL. With coherent ICS, FEL gain can occur with resulting improvements in the flux and brilliance of the x-ray beam. FEL gain in a laser undulator is observed with modest bunch charge and low currents given the proper electron beam modulation and emittance at the interaction point (IP). We present PIC simulations for the production of these nanobunched electron beams generated via emittance exchange (EEX). The generated electron beam is suitable for an XFEL based on the collision of a low energy electron beam with an IR or THz laser pulse producing a very compact and inexpensive x-ray laser.

To produce an electron bunch that has nanostructure we consider requirements at both the IP and at the cathode. The initial emittance for a metal cathode scales as 0.5×10^{-6} m-rad per mm rms spot size [3], therefore to produce 10^{-8} m-rad emittance for the electron bunch requires $\sigma_{x,y} = 20 \mu\text{m}$ at the cathode. The blowout mode, used to produce an ellipsoidal electron distribution [4], requires a laser spot with parabolic spatial intensity profile and a $40 \mu\text{m}$ edge radius. The initial charge density of $Q/\pi r^2 = 100 \text{ pC}/\text{mm}^2$ should be high enough to cause the bunch to expand significantly from its initial length but should remain below the space charge limit of $\epsilon_0 E_{\text{RF}} \sin(60^\circ) = 1100 \text{ pC}/\text{mm}^2$ at a cath-

ode peak field $E_{\text{RF}} = 150 \text{ MV}/\text{m}$. At an initial RF phase of 60° an un-chirped electron beam exits the gun.

A patterned photo-cathode consisting of a photo-field emitter array is used to generate the modulated electron beam. Various structures have been investigated theoretically and experimentally [5, 6] with Au ridges discussed presently. These vertical stripes of metal emitter are separated by non-emitting silicon dioxide coated areas. These ridges or lines provide the advantage of patterning the electron beam in only one dimension, which is effective because the EEX occurs with one transverse dimension [7, 8] and this reduces the electron density at the cathode. The EEX beamline will convert the electrons emitted from each metal stripe into a single beamlet that is less than half of the x-ray wavelength. Additionally, the pitch of the ridges can be fabricated on the order of 100 nm which helps limit the amount of demagnification needed to reach higher energies of radiation in the XFEL. The modulated electron bunch can be described with a parameter, known as the bunching factor, that is defined as

$$b_0 = \frac{1}{N_e} \sum_{p=1}^{N_e} e^{ikz_p} \quad (1)$$

where N_e is the number of electrons, z_p is the location of the p^{th} particle, $k = 2\pi/\lambda_x$, and λ_x is the period of modulation. A target bunching factor $b_0 = 0.3$ produces a significant coherent x-ray output and is achieved when each beamlet forms a nanobunch with rms length $\sigma_z^b = \lambda_x/4$. The metal stripe width must create a beamlet with transverse normalized emittance that is consistent with that bunch length while also keeping its energy spread below the FEL parameter, ρ_{FEL} . This means the beamlet must have emittance of

$$e_{xn}^b = \beta\gamma\sigma_z^b\sigma_E/E < \beta\gamma\rho_{\text{FEL}}\lambda_x/4 \text{ [m-rad]}. \quad (2)$$

In this expression the transverse emittance of a stripe at the cathode is equated with the longitudinal beamlet emittance downstream of the EEX at the IP.

RF STRUCTURES

A CAD layout of the modeled EEX LINAC is shown in Fig. 1 and consists of 3 RF structures – gun, LINAC, and RF deflector – all operating at 9.3 GHz and capable of managing the thermal load from a 1 kHz repetition rate. The RF structures were developed in collaboration with the High Power Microwave group at SLAC. The 2.5 cell X-band gun is optimized for high efficiency, high electric field at the emitter and low field in the coupling cell. SUPERFISH and HFSS models produce a 150 MV/m gradient at the emitter for 2 MW of RF power and a resulting beam energy of

* Supported by DARPA N66001-11-1-4192, DOE DE-FG02-10ER46745, DOE DE-FG02-08ER41532, and NSF DMR-1042342.

[†] enanni@mit.edu

2.1 MeV. The surface field on the emitter is maximized in order to minimize the effect of space charge on the emitted bunch. The fill time is 100 ns allowing short RF pulses to be used, and enabling a high repetition rate. The absolute value of the electric field in the gun is shown in Fig. 2(a) with the output slice emittance shown in Fig. 2(b). The initial projected emittance for the electron bunch was 8.5 nm-rad for 0.5 pC. With a final emittance of 9.1 nm-rad we see the excellent performance of the blowout mode with effectively no emittance growth. Two solenoids, found just downstream of the gun, with equal strength but opposite polarity focus the beam without causing rotation about the z-axis. The electron bunch is then passed through a 1 m LINAC which operates with a gradient of 20 MV/m and 20 MeV energy gain for 3 MW of input power.

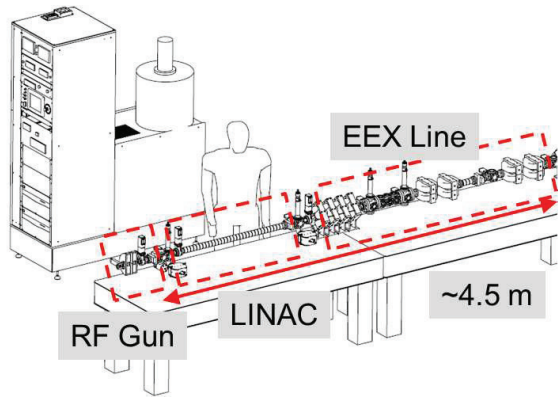


Figure 1: CAD layout of the 2-20 MeV EEX LINAC.

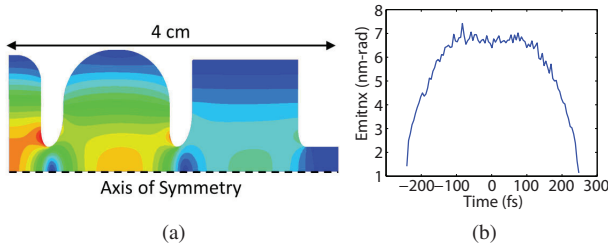


Figure 2: (a) Magnitude of the electric field in 2.5 cell RF gun and (b) the slice emittance at the exit of the RF gun.

The performance of the RF gun with a patterned photo-emitter was investigated, including space charge forces, for 0.5 pC electron bunches and spacings on the emitter as small as 100 nm. The subsequent components naturally demagnify this spacing by a factor of ~ 20 . Therefore, a modulation on the order of 10 nm, which corresponds to the emitted x-ray wavelength, is achievable with this setup at the IP. The emittance of an individual stripe when emitted from the cathode is 5.7 pm-rad, with the transverse phase space shown in Fig. 3(a). This emittance is significantly smaller than that of the whole bunch because of the reduction in the spatial extent, whereas the emitted angles remain the same. Due to the large divergence of the electrons at emission, the charge density in the transverse plane becomes uniform within several microns of the emitter (i.e. the transverse pattern is out of focus). Both 3D and ring space charge algo-

gorithms were investigated which minor differences observed, because of the absence of charge density fluctuations, except at image planes. At the exit of the gun the emittance for the central beamlet is 6.5 pm-rad, which leads to the observation that the blowout mode is well suited for maintaining the emittance not only of the global electron bunch, but also the beamlet. The electron distribution at the exit of the RF gun is shown in Fig. 3(b).

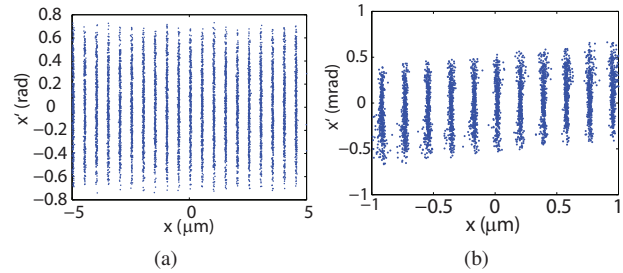


Figure 3: (a) Transverse modulations at the emitter surface and (b) at the exit of the electron gun, with individual electrons marked with dots. The phase space at the gun exit was sheared to remove a linear correlation in $x-x'$.

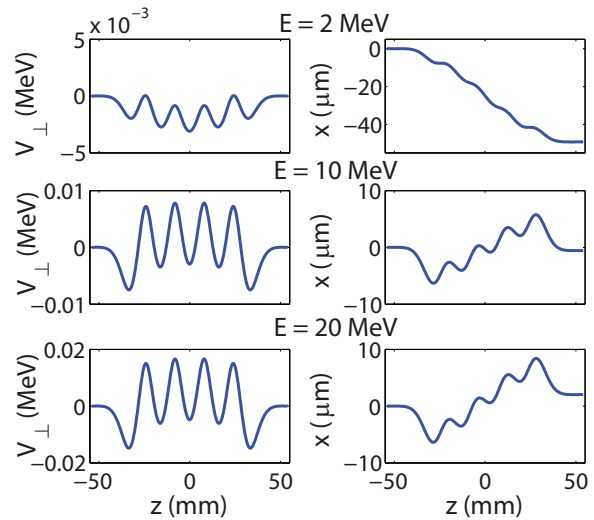


Figure 4: Transverse momentum as a function of distance for the reference zero-crossing particle and the transverse offset in the deflector cavity. The deflector cavity strength at 2, 10 and 20 MeV corresponds to a $V_{\perp}^{\max} = 0.07, 0.35$ and 0.7 MeV, respectively.

A 5 cell deflector cavity, with a standing wave mode to minimize the required RF power, was designed for use in the EEX line. Due to the low-energy electron beam, unique design features were included in the deflector to minimize the transverse offset at zero crossing. Additionally, the cavity was optimized to operate over the 2-20 MeV range accessible by the LINAC. The TM_{110} mode is excited by two couplers located in the center cell. The transverse shunt impedance, defined as

$$R_T = \frac{\left| \int_0^{L_c} (cB_x + E_y) e^{j\omega_{RF}z/c} dz \right|^2}{2P} \quad (3)$$

Table 1: Deflector Parameters

Number of Cells	R_T Single Cell [M Ω /m]	Q_L	V_{\perp}	P_{IN}	E_{max}	H_{max}
5	0.3502	5000	0.7 MeV	200 kW	32 MeV/m	112 kA/m

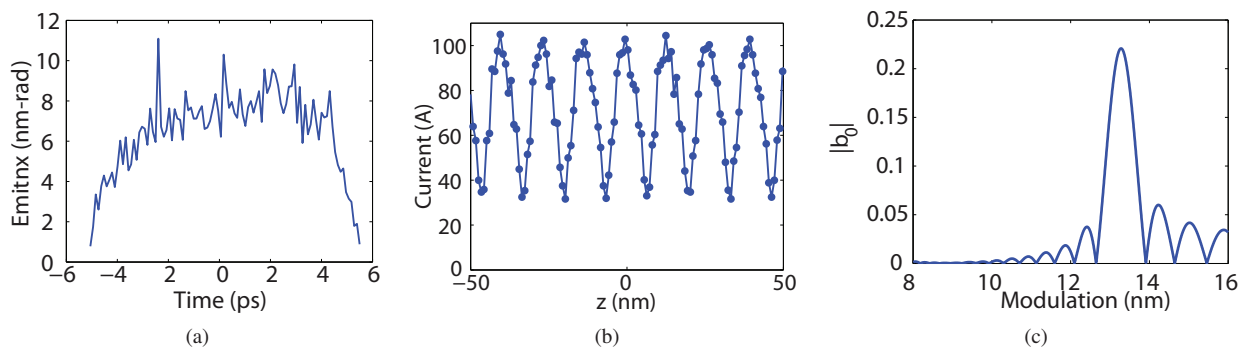


Figure 5: (a) Slice Emittance at the IP for the global bunch with the deflector off. The (b) modulated current and (c) bunching factor at the IP after EEX with the deflector on.

determines the effectiveness of the deflector cavity. The design parameters for the deflector are shown in Table 1. For EEX the deflector cavity operates at zero crossing imparting opposite kicks to the leading and trailing particles. Under a thin lens approximation the deflector cavity does not produce a transverse offset for the reference particle at zero crossing. However, due to the finite length of the cavity the reference particle would traverse the deflector cavity with a non-zero mean transverse momentum. In order to mitigate this each of the cavity end cells provides half the kick of a full cell. This effectively results in a zero mean transverse momentum for a single optimized energy. In Fig. 4 the transverse particle momentum and offset are shown for the reference particle at three energies (2, 10, 20 MeV) covering the full range accessible by the LINAC. The final transverse momentum for all three cases is zero due to proper phasing of the reference particle. However, the mean transverse momentum is non-zero for the 2 and 20 MeV case. This is demonstrated by the non-zero axial offset for the particle at the exit of the cavity.

EEX LINE

After the LINAC, a group of 2 quadrupole doublets matches the transverse phase space into the EEX line to provide upright longitudinal ellipses downstream at the IP. The EEX line consists of 2 doglegs, each with dispersion of 18.97 cm, separated by the RF deflector. Following the EEX line another group of 2 quadrupole doublets focuses the electron beam at the IP. The doublets are designed to provide a β^* at the IP as low as 0.2 mm. The slice emittance at the end of the setup for the full electron bunch at 20 MeV is shown in Fig. 5(a) with the deflector cavity off for comparison with Fig. 2(b). With a beamlet emittance of 15 pm-rad, determined by the beamlet rms size $\sigma_x^b = 28.9$ nm at the photo-cathode, the EEX line can produce 13 nm modula-

tion at the IP. The modulation period can be reduced with a smaller initial emittance or σ_x^b . Fig. 5(b) shows the current at the IP for a 100 nm segment of the bunch. The bunching factor calculated as a function of modulation period for the entire electron bunch is shown in Fig. 5(c). The emitted photon flux scales as $(b_0 N_e)^2$ for coherent emission [1] and N_e for incoherent emission resulting in an increase in flux of $\sim 10^4$ for 0.5 pC.

CONCLUSION

We have presented the design and simulation of a compact LINAC capable of producing a modulated electron beam on the nanometer scale that is suitable for producing a coherent x-ray beam when scattered from a laser undulator. The entire accelerator and transport line is less than 5 m long and consists of a small number of components. The very stable optical, thermal, mechanical, and electrical requirements can be met at modest cost due to the small size. The electron energy is so low that synchrotron radiation effects on the beam are negligible. Although care is needed in handling and transport of the low energy beam, the short accelerator simplifies the physics and has significant advantages over a large machine. The electron beam parameters meet the requirements for FEL gain.

ACKNOWLEDGMENT

The design of the LINAC RF structure and significant aspects of the photoinjector cavity design were performed by Sami Tantawi and Valery Dolgashev of SLAC.

REFERENCES

- [1] Graves, W. S., et al. "Intense superradiant x rays from a compact source using a nanocathode array and emittance exchange." *Physical Review Letters* 108.26 (2012): 263904.

Content from this work may be used under the terms of the CC BY 3.0 licence (© 2014). Any distribution of this work must maintain attribution to the author(s), title of the work, publisher, and DOI.

- [2] Graves, W. S., et al. "Compact XFEL Light Source." Proceedings of the 2013 FEL Conference, New York, USA, 2013.
- [3] Dowell, David H., and John F. Schmerge. "Quantum efficiency and thermal emittance of metal photocathodes." Physical Review Special Topics-Accelerators and Beams 12.7 (2009): 074201.
- [4] Luiten, O. J., et al. "How to realize uniform three-dimensional ellipsoidal electron bunches." Physical Review Letters 93.9 (2004): 094802-094802.
- [5] Swanwick, M. E., et al. "Nanostructured silicon photocathodes for x-ray generation." Vacuum Nanoelectronics Conference (IVNC), 2013 26th International. IEEE, 2013.
- [6] Hobbs, R. G., et al. "High-density optically actuated Au nanorod electron emitter arrays." Vacuum Nanoelectronics Conference (IVNC), 2013 26th International. IEEE, 2013.
- [7] Cornacchia, M. and P. Emma, Physical Review Special Topics-Accelerators and Beams 5, 084001 (2002).
- [8] Emma, P., Z. Huang, K.-J. Kim, and P. Piot, Physical Review Special Topics-Accelerators and Beams 9, 100702 (2006).